A mechanical analysis of woodpecker drumming and its application to shock-absorbing systems

2011 Bioinspir. Biomim. 6 016003

(http://iopscience.iop.org/1748-3190/6/1/016003)

Bioinsp. Biomim. **6** (2011) 016003 (12pp) doi:10.1088/1748-3182/6/1/016003

A mechanical analysis of woodpecker drumming and its application to shock-absorbing systems

Sang-Hee Yoon[1,2,3] **and Sungmin Park**[2]

[1] Molecular Cell Biomechanics Laboratory, Department of Bioengineering, University of California, Berkeley, CA 94720, USA
[2] Department of Mechanical Engineering, University of California, Berkeley, CA 94720, USA

E-mail: sang-hee.yoon@wyss.harvard.edu

Received 28 July 2010
Accepted for publication 16 December 2010
Published 17 January 2011
Online at stacks.iop.org/BB/6/016003

Abstract

A woodpecker is known to drum the hard woody surface of a tree at a rate of 18 to 22 times per second with a deceleration of 1200 *g*, yet with no sign of blackout or brain damage. As a model in nature, a woodpecker is studied to find clues to develop a shock-absorbing system for micromachined devices. Its advanced shock-absorbing mechanism, which cannot be explained merely by allometric scaling, is analyzed in terms of endoskeletal structures. In this analysis, the head structures (beak, hyoid, spongy bone, and skull bone with cerebrospinal fluid) of the golden-fronted woodpecker, *Melanerpes aurifrons*, are explored with x-ray computed tomography images, and their shock-absorbing mechanism is analyzed with a mechanical vibration model and an empirical method. Based on these analyses, a new shock-absorbing system is designed to protect commercial micromachined devices from unwanted high-*g* and high-frequency mechanical excitations. The new shock-absorbing system consists of close-packed microglasses within two metal enclosures and a viscoelastic layer fastened by steel bolts, which are biologically inspired from a spongy bone contained within a skull bone encompassed with the hyoid of a woodpecker. In the experimental characterizations using a 60 mm smoothbore air-gun, this bio-inspired shock-absorbing system shows a failure rate of 0.7% for the commercial micromachined devices at 60 000 *g*, whereas a conventional hard-resin method yields a failure rate of 26.4%, thus verifying remarkable improvement in the *g*-force tolerance of the commercial micromachined devices.

(Some figures in this article are in colour only in the electronic version)

1. Introduction

A mechanical shock is known to seriously deteriorate the linear operation of any spring–mass-type micromachined device and even to physically damage the micromachined device due to its frequency of more than 10 kHz (Chu 1988) and amplitude above 1000 *g* (Yazdi *et al* 1998). There has been an unceasing need for micromachined devices with improved *g*-force tolerance for use in high-*g* environments. Thus, a new shock-absorbing system for protecting micromachined devices from transient mechanical excitations is considered as one of the most challenging progresses in the nano/microelectromechanical system (N/MEMS) field (Veprik and Babitsky 2000, Britan *et al* 2001, Yoon and Kim 2006). Early effort to absorb incident mechanical excitations has been focused on *shock attenuators* (SAs) which damp all mechanical excitations over all frequencies. According to their working mechanism or material, previous SAs are classified into viscoelastic SAs (Nakra 1976, 1981, 1984, Grover and Kapur 1982), fluid SAs (Dareing and Johnson 1975, Ping 2007), and non-obstructive particle damping (NOPD) SAs (Panossian 1991, 1992, Friend

[3] Author to whom any correspondence should be addressed.

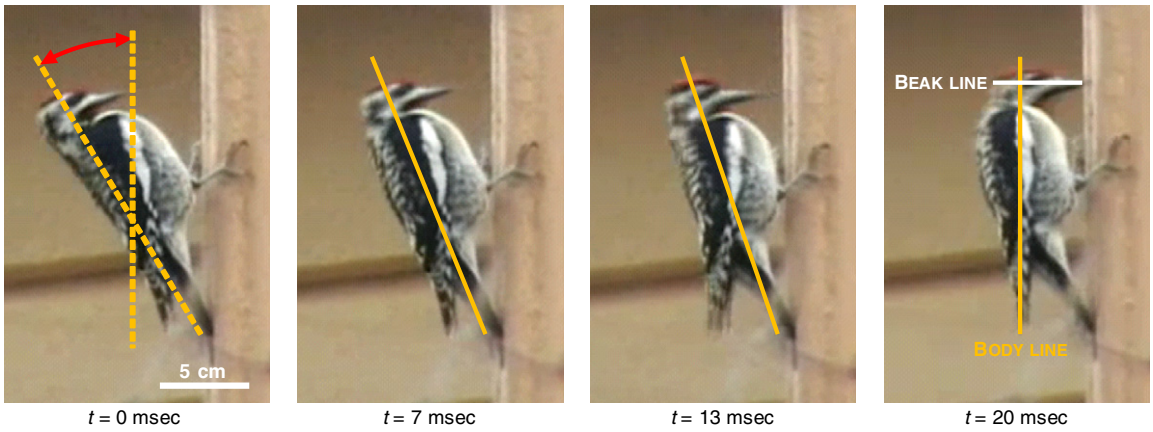

Figure 1. Time-sequential images of the red-bellied woodpecker, *Melanerpes carolinus*, showing its drumming pose. This bird drums a tree as fast as about 20 beats per second. On the drumming, the woodpecker keeps its beak (beak line) and body (body line) perpendicular and parallel to a wood, respectively. The relatively longer tail fits closely along the wood surface for balance. Photos courtesy of TomSlatin.com. See the video on http://www.tomslatin.com/confused-woodpecker.html.

and Kinra 2000). The viscoelastic SAs are severely degraded at low and high temperatures, yielding low performance in attenuating mechanical excitations (Nashif *et al* 1985); the fluid SAs which absorb incident mechanical excitations by means of heat and acoustic energies are too bulky to be incorporated into micromachined devices; the NOPD SAs which smooth out mechanical excitations through friction and momentum exchange between particles and wall cannot be used for micromachined devices, which are too small for holes to be made in them. The other shock-absorbing effort has been in *shock low-pass filters* which pass low-frequency mechanical excitations but attenuate high-frequency ones to protect micromachined devices. However, there have been almost no reports on it (Yoon and Kim 2006). Although the previous shock-absorbing systems showed fair performance, they suggested that there is still much scope to improve shock-absorbing systems for micromachined devices.

Nature causes some traits that aid survival and reproduction to become commoner, and makes other traits that hinder them to become rarer; all creatures in nature are believed to be perfectly equipped with biological features over successive generations through natural selection (Vogl 1998). Our engineers are therefore trying to find clues to solve problems arising in engineering by understanding natural creatures with advanced performance and high efficiency. In this paper, a woodpecker (family Picidae, order Piciformes) is intensively investigated as a biological example for the development of a new shock-absorbing system. People may be interested in the woodpecker and its peculiar drumming behavior and ask the question 'how does the bird strike its beak against a tree repeatedly without brain damage?' To find an answer, the bird's endoskeletal structures—beak, hyoid, spongy bone, and skull bone with cerebrospinal fluid (CSF)—are studied with x-ray computed tomography (CT) images and the secrets of each structure are explored in theoretical and experimental ways. The shock-absorbing mechanism of beak, hyoid, and skull bone with CSF is quantitatively explored in a theoretical way using simplified mechanical vibration theory, while that of spongy bone is investigated in an experimental way. From these analyses, a new shock-absorbing system inspired by a woodpecker is designed, fabricated, and characterized to avoid the performance deterioration and physical damage of micromachined devices from external mechanical excitations.

2. Biomimetic approach

2.1. Ecological characteristics of the woodpecker

A woodpecker is an interesting bird whose endoskeletal structures allow it to drill holes in wood, i.e., *drumming*. According to previous analyses on a woodpecker's drumming (May *et al* 1976a, 1976b, Stark *et al* 1998, Schwab 2002), most of woodpecker species drum a tree at an amazing speed of about 20 beats per second and a deceleration of 1200 g without brain damage (brain concussion) and even *g*-force induced loss of consciousness (G-LOC). For example, the ladder-backed woodpecker, *Picoides scalaris*, strikes a tree as fast as 28.4 beats per second, and this drumming is repeated 500 to 600 times per day.

Prior to a detailed discussion about anatomic features of the woodpecker closely associated with drumming motion, the drumming pose of a woodpecker needs to be addressed. When a woodpecker drums a tree, its beak (white line in figure 1, beak line) and body (yellow line in figure 1, body line) are respectively perpendicular and parallel to the tree and its head does not rotate in a 'yes–no' manner during drumming. This drumming pose therefore greatly reduces the shear force on its brain, which is known to cause G-LOC and to be more harmful to brain tissues (May *et al* 1976a, 1976b). As shown in figure 1, the time-sequential images of the drumming motion of the red-bellied woodpecker (*Melanerpes carolinus*) demonstrate that the mechanical excitations exerted by drumming are not shear forces but horizontal ones.

2.2. Endoskeletal structures of the woodpecker

A woodpecker is known to be equipped with remarkable endoskeletal and tissue characteristics to protect its brain

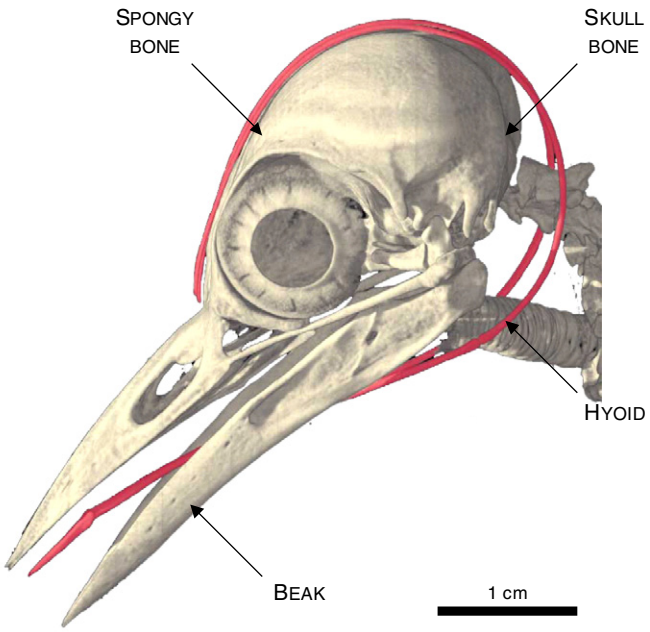

Figure 2. Head structures of the golden-fronted woodpecker, *Melanerpes aurifrons*, showing its beak, hyoid (highlighted in red), spongy bone, and skull bone with cerebrospinal fluid. The spongy bone, a part of the skull bone, is located in the forepart of the skull bone. Photo courtesy of Digital Morphology, which is available at http://digimorph.org/specimens/Melanerpes_aurifrons/.

from incident mechanical excitations. A clear understanding of these characteristics will therefore lead to the successful design of a new shock-absorbing system for micromachined devices. Based on the x-ray CT images of the golden-fronted woodpecker, *Melanerpes aurifrons*, (DigiMorph Staff 2004), a woodpecker's head structures of beak, hyoid, spongy bone, and skull bone with CSF were intensively studied to elucidate its special anatomy. Figure 2 shows the head structure of a woodpecker. The woodpecker has a relatively long, heavy, and rigid tail compared to other birds (see figure 1). During drumming, the woodpecker aligns the tail along a tree to keep its balance and to maintain its drumming pose on the tree. Tail feathers, which are known to resist wear caused by their use in propping up the body during drumming, are also stiffer than those of other birds' (Gibson 2006). Although the tail and its features are necessary to keep the drumming pose, they are believed to absorb only a very small amount of incident mechanical excitations. Their shock-absorbing effect is therefore not considered in this paper.

The woodpecker's beak (figures 2 and 3) is a specialized chisel effective in cutting into a tree; unlike a human-made chisel, the beak is self-sharpening (May *et al* 1976a, 1976b, Schwab 2002, Oda *et al* 2006); the beak, made of elastic material, is relatively large compared to the body. This endoskeletal feature prevents incident mechanical excitations of drumming from directly reaching the brain. The third feature is a hyoid which rigidly supports the tongue. This musculotendinous tissue serves as an attachment site for the muscles around the throat and tongue. The hyoid extends posteriorly from the floor of mouth, goes behind the neck, divides into two bands, encompasses the head, and comes forward to the nostril, as highlighted in red in figures 2 and 3 (May *et al* 1976a, 1976b, Moore and Dalley 2005). This feature, not seen in other birds, aids the woodpecker in extending its tongue in order to evenly distribute incident mechanical excitations from drumming and to reinforce the head—in other words, the hyoid bypasses the vibrations generated from drumming. A spongy bone, which is specially located at the contrecoup position from the beak, allows the woodpecker to avoid brain damage (May *et al* 1976a, 1976b). This bone is relatively dense but spongy compared to other bones, as shown in figures 2 and 3. The spongy bone is thought to evenly distribute incident mechanical excitations before they propagate to the brain. Although this feature was revealed in 1976 (May *et al* 1976a), almost nothing was known about its shock-absorbing characteristics. Finally, a skull bone with CSF plays also a key role in dissipating mechanical excitations from drumming. As shown in figure 3, the woodpecker has a very narrow space for CSF between the skull bone and brain. This bird therefore has a relatively little CSF, thereby reducing the transmission of the mechanical excitations into the brain through the CSF (May *et al* 1976a, 1976b, Schwab 2002).

Using the above endoskeletal features of the beak, hyoid, spongy bone, and skull bone with CSF, a woodpecker can protect its head from damage. Without these endoskeletal features, this bird might be killed by drumming impact. To devise a new shock-absorbing system for micromachined devices, the shock-absorbing mechanism of the beak, hyoid, and skull bone with CSF are theoretically analyzed with a simplified mechanical vibration model, whereas that of the spongy bone is empirically characterized.

3. Analysis of the drumming motion

3.1. Allometric analysis

The first analysis was an allometric approach for calculating the *g*-force tolerance of a woodpecker, compared to that of a human. Allometry is effective in describing a scaling effect (that is, a relationship between organism size and its organ size) such that it is used to determine whether the shock-absorbing mechanism of the woodpecker is the result of its small size or not.

Assuming that the same yield stress S_y is acting on the brains of the woodpecker and human, the *g*-force tolerance of a woodpecker is compared with that of a human,

$$S_{y,w} = \frac{m_w a_w}{A_w} = \frac{m_h a_h}{A_h} = S_{y,h}, \tag{1}$$

where m, a, and A are the mass, deceleration, and cross-sectional area of the brain. The subscripts of w and h represent the woodpecker and human, respectively. The *g*-force tolerance of the woodpecker is written as

$$a_w = \frac{m_h A_w}{m_w A_h} a_h = 13.1 a_h. \tag{2}$$

The *g*-force tolerance of the woodpecker, calculated from equation (2) with the parameters summarized in table 1, was about 13 times larger than that of the human. A human is known to lose consciousness at a *g*-force of 4 to 6 *g*

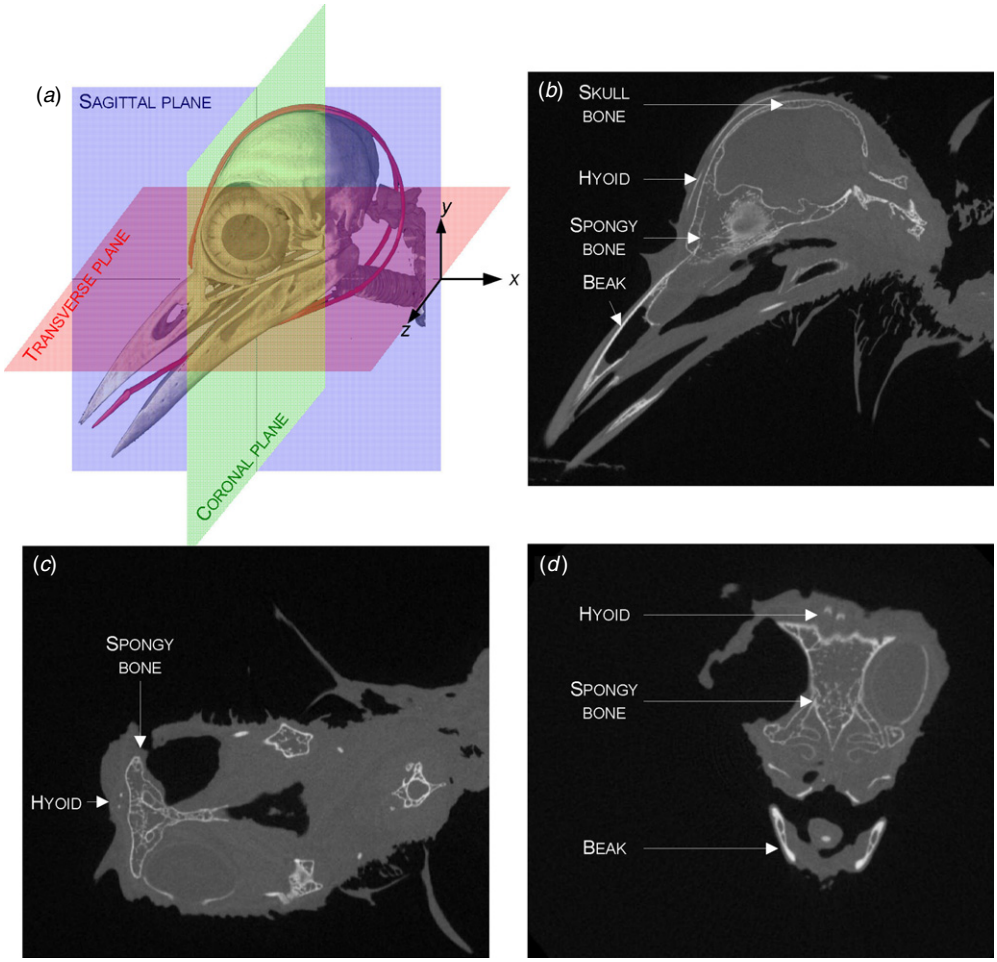

Figure 3. X-ray computed tomography (CT) images of the head structure of the golden-fronted woodpecker, showing the beak, hyoid, spongy bone, and skull bone. (*a*) 3D visualization from CT scan images. (*b*) Sagittal slice view. (*c*) Transversal slice view. (*d*) Coronal slice view. Photo courtesy of Digital Morphology, which is available at http://digimorph.org/specimens/Melanerpes_aurifrons/.

Table 1. Parameters used in the allometric analysis.

Parameter	Human[a]	Woodpecker
Mass (kg)	1.40 (female), 1.50 (male)	1.00×10^{-3}[b]
Diameter (cm)	12.9 (female), 13.4 (male)	1.25[c]

[a] Parent 1996.
[b] Vincent *et al* 2007.
[c] Measured from the slice image of the golden-fronted woodpecker of the Digital Morphology Library.

(9 *g* with g-suit) (Burton 1988, Whinnery and Whinnery 1990), indicating a woodpecker will have its G-LOC at a deceleration of about 65.5 *g*. A woodpecker, however, is known to avoid brain damage and even G-LOC from sudden deceleration as high as 1200 *g* on each impact (Vincent *et al* 2007, Schwab 2002). This allometric analysis suggests that a woodpecker has its own advanced shock-absorbing mechanism which cannot be explained merely by allometric scaling.

3.2. Mechanical vibration analysis

A simplified mechanical vibration model is prepared from the kinematics of a woodpecker to analyze its special shock-absorbing mechanism, as shown in figure 4(*a*). When the woodpecker strikes its beak against a tree, its endoskeletal structures (beak, hyoid, spongy bone, and skull bone with CSF) stand in a row to sequentially absorb the mechanical excitations generated by drumming. A simplified mass–damper–spring lumped parameter model for the woodpecker's head is prepared with the following assumptions: (i) a woodpecker rotates about its center of rotation (figure 4(*a*)); (ii) while drumming, the beak (beak line in figure 1) and body (body line in figure 1) are perpendicular and parallel to the tree, respectively; (iii) the beak is described as a lumped parameter model composed of one mass and two Kelvin models; (iv) the hyoid and skull bone are modeled as lumped parameter models composed of one mass and one Kelvin model, respectively; (v) the spongy bone is not considered here due to its complexity in modeling. The shock absorption of a woodpecker drumming a tree is modeled with the lumped parameters of mass, damper, and spring to express a multi-degree-of-freedom motion, as shown in figure 4(*b*). The equations of motion can be obtained by using the Lagrange equation of motion in the following form,

$$m\ddot{x} + c\dot{x} + kx = F(t), \tag{3}$$

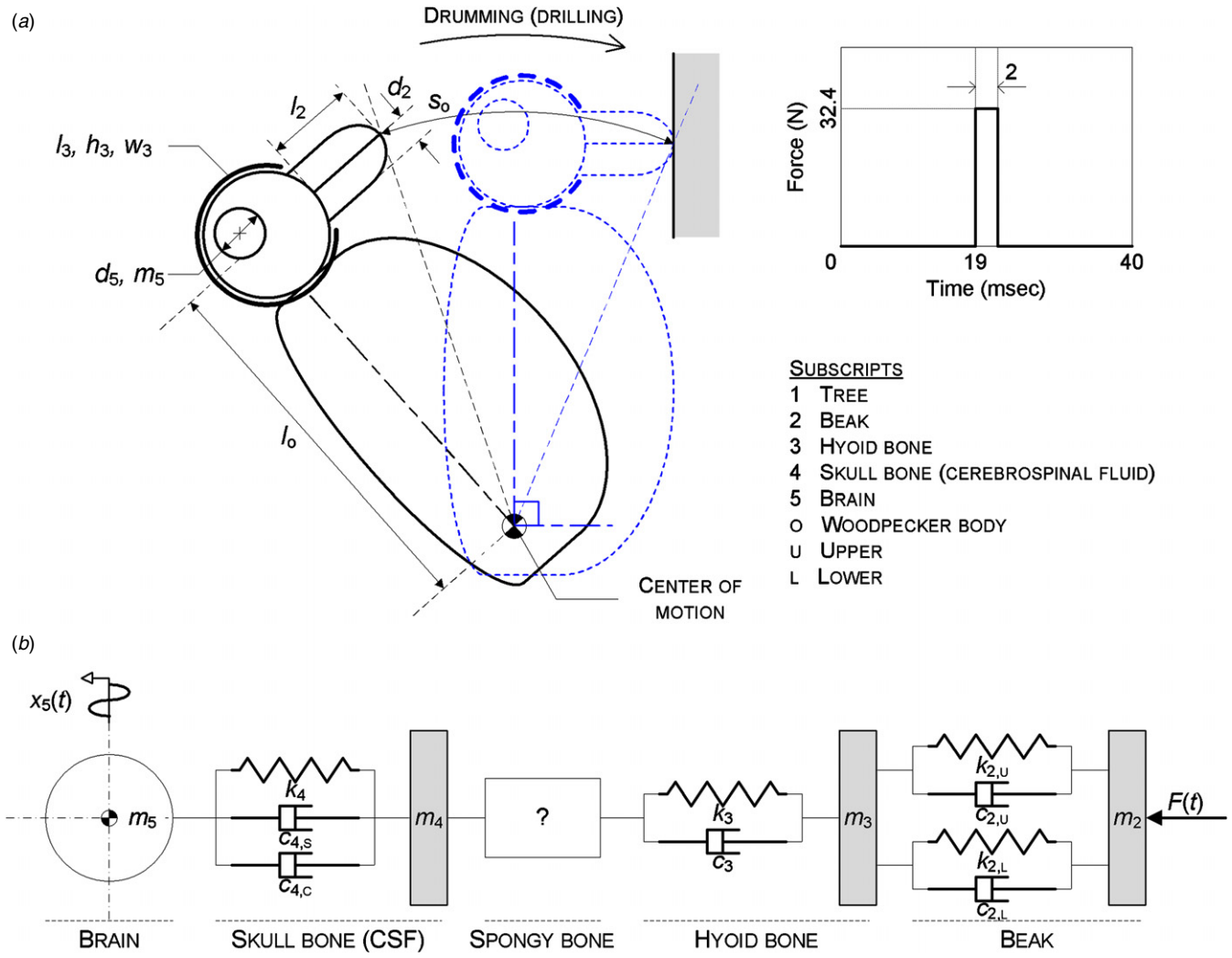

Figure 4. Simplified model of a woodpecker. (*a*) Kinematic model of the woodpecker's drumming motion. (*b*) Mass–damper–spring model of the head of a woodpecker which drums a tree.

where m, c, and k are respectively the mass, damping coefficient, and stiffness of an object whose displacement is x under external force F. Without considering the spongy bone which will be analyzed in an empirical way later, the mass–damper–spring model of the woodpecker's head is equivalently simplified as a four-degree-of-freedom system, as shown in figure 5. This equivalent mass–damper–spring model is expressed as

$$\begin{bmatrix} m_2 & 0 & 0 & 0 \\ 0 & m_3 & 0 & 0 \\ 0 & 0 & m_4 & 0 \\ 0 & 0 & 0 & m_5 \end{bmatrix} \begin{bmatrix} \ddot{x}_2 \\ \ddot{x}_3 \\ \ddot{x}_4 \\ \ddot{x}_5 \end{bmatrix} + \begin{bmatrix} c_1 + c_2 & -c_2 & 0 & 0 \\ -c_2 & c_2 + c_3 & -c_3 & 0 \\ 0 & -c_3 & c_3 + c_4 & -c_4 \\ 0 & 0 & -c_4 & c_4 \end{bmatrix} \begin{bmatrix} \dot{x}_2 \\ \dot{x}_3 \\ \dot{x}_4 \\ \dot{x}_5 \end{bmatrix} + \begin{bmatrix} k_1 + k_2 & -k_2 & 0 & 0 \\ -k_2 & k_2 + k_3 & -k_3 & 0 \\ 0 & -k_3 & k_3 + k_4 & -k_4 \\ 0 & 0 & -k_4 & k_4 \end{bmatrix} \begin{bmatrix} x_2 \\ x_3 \\ x_4 \\ x_5 \end{bmatrix} = \begin{bmatrix} F(t) \\ 0 \\ 0 \\ 0 \end{bmatrix}, \tag{4}$$

where the subscripts of 1, 2, 3, 4, and 5 represent a tree, the beak, hyoid, skull bone with CSF, and brain of a woodpecker, respectively. The displacement of the brain $x(t)$ under drumming impact $F(t)$ is calculated by solving equation (4) after determining the external force of $F(t)$, the initial conditions of $\dot{x}_i(0)$ and $x_i(0)$, and the coefficients of m_i, c_i, and k_i.

A woodpecker is known to produce a striking velocity v_s of 3.6 m s^{-1} over a drumming distance s_o of 7×10^{-2} m when the bird drums a tree at a frequency f_d of 25 Hz (Stark *et al* 1998, Vincent *et al* 2007). Thus, the time for single drumming

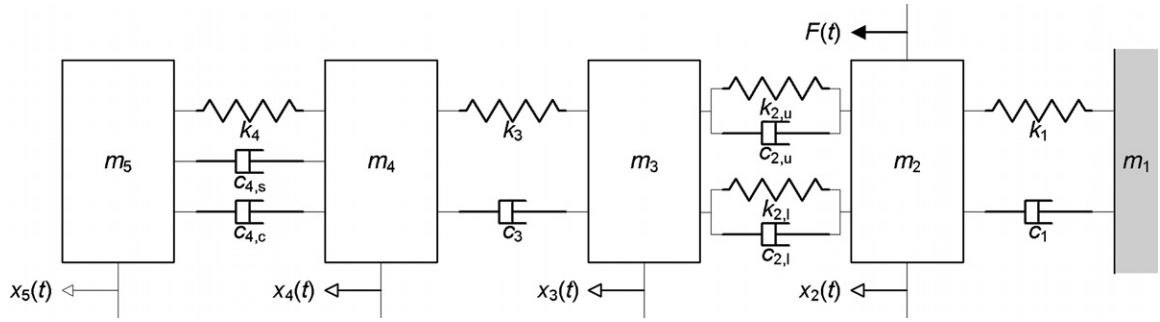

Figure 5. Equivalent mass–damper–spring model of the head structure of a woodpecker without considering the spongy bone.

is $t_d = 1/f_d = 0.04$ s. Assuming a forward drumming has the same velocity with a backward one, the time for forward or backward drumming t_m is given by

$$t_m = s_o/v_s = 0.019 \text{ s}. \tag{5}$$

The time between forward and backward drummings t_p, when the woodpecker penetrates the tree with its beak, is therefore represented by

$$t_p = t_d - 2t_m = 0.002 \text{ s}. \tag{6}$$

From a linear momentum equation, the external force $F(t)$ is described as

$$F(t) = \frac{\Delta P}{t_p} = \frac{2m_h v_s}{t_p}, \tag{7}$$

where ΔP is a change in the linear momentum at drumming and m_h is the head mass of a woodpecker, 9×10^{-3} kg (Vincent *et al* 2007). The external force $F(t)$ is therefore written as

$$\begin{aligned} F(t) &= 32.4 \text{ N} \quad (0 \leqslant t < 0.002), \\ &0 \quad \text{N} \quad (\text{otherwise}). \end{aligned} \tag{8}$$

Assuming an initial displacement of 0 m and an initial velocity of -3.6 m s^{-1} (striking velocity), the initial conditions will be expressed as

$$\begin{aligned} &\dot{x}_2(0) = \dot{x}_3(0) = \dot{x}_4(0) = \dot{x}_5(0) = -3.6 \text{ ms}^{-1}, \\ &x_2(0) = x_3(0) = x_4(0) = x_5(0) = 0 \text{ m}. \end{aligned} \tag{9}$$

The coefficients of m_i, c_i, and k_i are obtained from the geometry and material properties of the endoskeletal structures of the woodpecker. The coefficients of the tree, denoted by the subscript 1, are determined as $c_1 = 10$ N s m^{-1} and $k_1 = 1000$ N m^{-1} from previous research (Moore and Maguire 2004). To model the beak into lumped parameters, the upper and lower beaks are assumed as two cylinders with a diameter d_2 of 6×10^{-3} m and a length l_2 of 2.6×10^{-2} m, which are measured from the x-ray CT images of the woodpecker (DigiMorph Staff 2004). Due to a shortage of information on beak density ρ_2, a bird's cranium density of 1456 kg m^{-3} (Oda *et al* 2006) is used in this analysis. The mass of the beak m_2 is calculated as

$$m_2 = 2\rho_2 \cdot \pi (d_2/2)^2 \cdot l_2 = 2.1 \times 10^{-3} \text{ kg}. \tag{10}$$

The stiffness of the beak k_2 from solid mechanics is given by

$$k_2 = k_{2,\mathrm{ub}} + k_{2,\mathrm{lb}} = \frac{2A_2 \cdot E_2}{l_2}, \tag{11}$$

where A_2 and E_2 are the cross-sectional area and Young's modulus of the beak, and the subscripts ub and lb denote upper beak and lower beak, respectively. Because there is no published data on Young's modulus of the beak, that of a toucan beak (30 MPa, Seki *et al* 2005) is used, thereby yielding $k_2 = 6.5 \times 10^4$ N m^{-1}. The damping coefficient of the beak c_2 is obtained from that of a human bone with the damping coefficient of $\tan\delta = 0.032$ (Fortis *et al* 2004). Thus, the damping coefficient of the beak is calculated as

$$c_2 = c_{2,\mathrm{ub}} + c_{2,\mathrm{lb}} = \tan\delta\sqrt{m_2 \cdot k_2} = 0.37 \text{ N s m}^{-1}. \tag{12}$$

The woodpecker's hyoid is assumed as two curved parallelepipeds whose length l_3, height h_3, and width w_3 are 66.7×10^{-3}, 6.5×10^{-4}, and 6.5×10^{-4} m, respectively, obtained from the x-ray CT images of the woodpecker (DigiMorph Staff 2004). Considering that the hyoid is almost the same with a tendon, the hyoid is assumed to have a density ρ_3 of 1200 kg m^{-3} (Oda *et al* 2006) and Young's modulus E_3 of 1.5 GPa (Alexander and Bennet-Clark 1977). The total mass of the hyoid m_3 is represented as

$$m_3 = 2\rho_3 \cdot l_3 \cdot h_3 \cdot w_3 = 67.6 \times 10^{-6} \text{ kg}. \tag{13}$$

The stiffness of the hyoid k_3 is estimated by using the same method above, described as

$$k_3 = \frac{2l_3 \cdot w_3 \cdot E_3}{h_3} = 2.0 \times 10^8 \text{ N m}^{-1}. \tag{14}$$

The damping coefficient of the hyoid c_3 is also estimated from that of the human tendon with a damping ratio of $\zeta = 0.25$ (Revel *et al* 2003), written as

$$c_3 = \zeta\sqrt{m_3 \cdot k_3} = 5.63 \text{ N s m}^{-1}. \tag{15}$$

The skull bone with CSF is regarded as a thin-walled sphere with a diameter d_4 of 2×10^{-2} m and a thickness t_4 of 2.5×10^{-3} m, obtained from the x-ray CT images (DigiMorph Staff 2004), and is modeled as one mass m_4, two dampers $c_{4,\mathrm{s}}$, $c_{4,\mathrm{c}}$, and one spring k_4. The mass of skull bone m_4 is calculated as

$$m_4 = \rho_4 \cdot 4\pi (d_4/2)^2 \cdot t_4 = 4.6 \times 10^{-3} \text{ kg}, \tag{16}$$

where ρ_4 is the density of the skull bone whose published values is 1456 kg m^{-3} (Oda *et al* 2006). Focusing on the regime of linear deformation, the stiffness of skull bone k_4 can

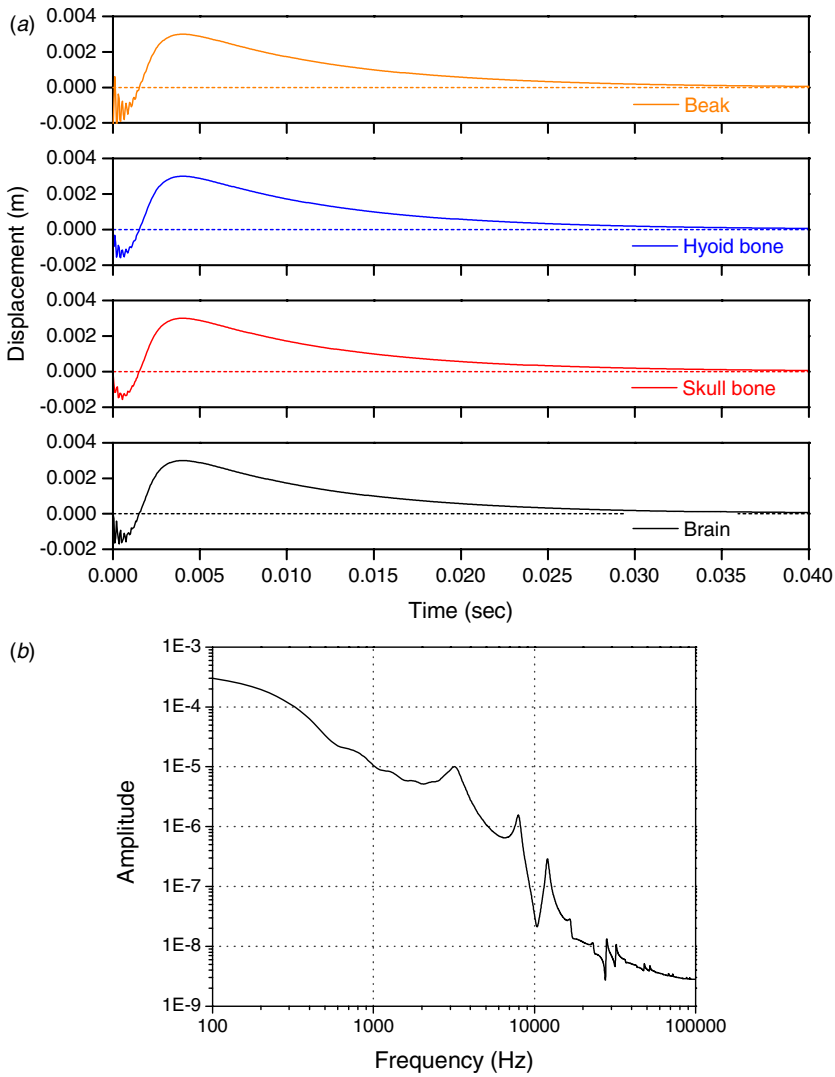

Figure 6. Mechanical vibration analysis of a woodpecker (beak, hyoid, skull bone, and brain) under drumming impact without considering the spongy bone. (*a*) Dynamic response. (*b*) Frequency spectrum diagram of the dynamic response of a brain. The relatively high-frequency vibrations of the brain during $t = 0$ to 2 ms, which can cause g-force-induced loss of consciousness or brain damage to the woodpecker, indicate that the spongy bone eliminates the initial high-frequency vibrations as a mechanical low-pass filter.

be expressed by that of a thin spherical shell undergoing small deformation (Reissner 1946, Koiter 1963),

$$k_4 = \frac{2E_4}{\sqrt{3(1-\upsilon^2)}}\frac{t_4^2}{d_4} = 3.2 \times 10^6 \text{ N m}^{-1}, \tag{17}$$

where E_4 and υ are Young's modulus and Poisson's ratio of the skull bone whose values are 8.75 GPa and 0.2, respectively (Oda *et al* 2006). The damping of the skull bone with CSF c_4 is considered to be composed of the skull bone damping $c_{4,\text{s}}$ and the CSF damping $c_{4,\text{c}}$, given by

$$c_4 = c_{4,\,s} + c_{4,\,c} = \tan\delta\sqrt{m_4 \cdot k_4} + 3\pi\ \mu_4\, d_4 = 3.88 \text{ N s m}^{-1}, \tag{18}$$

where $\tan\delta$ is the damping coefficient of the skull bone and μ_4 is the viscosity of the CSF. Based on humans' data (Fortis *et al* 2004, Bloomfielda *et al* 1998), those are determined as 0.032 and 8.5×10^{-4} N s m^{-1}. The first is obtained using mechanical vibration theory, while the second is done using the Stokes equation. The last but not least, what we need is the brain mass of the woodpecker m_5, represented as

$$m_5 = \rho_5 \cdot \frac{4\pi}{3} \cdot \left(\frac{d_5}{2}\right)^3 = 1.8 \times 10^{-3} \text{ kg}, \tag{19}$$

where ρ_5 is the density of the brain which is known to be 1040 kg m^{-3} (Oda *et al* 2006) and d_5 is the diameter of the brain which is assumed to be 1.5×10^{-2} m, also measured from the x-ray CT images (DigiMorph Staff 2004). All parameters used in this analysis are summarized in table 2.

The displacements of the beak, hyoid, skull bone with CSF, and brain of a woodpecker under drumming impact are obtained by solving equations (4)–(19). Figure 6(*a*) shows the estimated dynamic responses of those head structures without considering the spongy bone. A frequency spectrum diagram of the dynamic response of the brain, as demonstrated in figure 6(*b*) indicates that there are relatively high-frequency vibrations during $t = 0$ to 2 ms, which may lead the woodpecker to G-LOC and even brain concussion. Since

Table 2. Parameters used in the mechanical vibration analysis.

Structure	Parameter	Symbol	Value	Reference
Woodpecker	Drumming distance	S_o	7×10^{-2} m	Vincent *et al* 2007
	Drumming frequency	f_d	25 Hz	Stark *et al* 1998, Vincent *et al* 2007
	Striking velocity	v_s	3.6 m s^{-1}	Vincent *et al* 2007
	Penetrating time[a]	t_p	2×10^{-3} sec	–
	Head mass	m_h	9×10^{-3} kg	Vincent *et al* 2007
Tree	Stiffness	k_1	1000 N m^{-1}	Moore and Maguire 2004
	Damping coefficient	c_1	10 N·s m^{-1}	Moore and Maguire 2004
Beak	Length	l_2	2.6×10^{-2} m	DigiMorph Staff 2004
	Diameter	d_2	6×10^{-3} m	DigiMorph Staff 2004
	Density[b]	ρ_2	1456 kg m^{-3}	Oda *et al* 2006
	Young's modulus[c]	E_2	3×10^7 Pa	Seki *et al* 1998
	Damping coefficient[d]	Tan δ	0.032	Fortis *et al* 2004
Hyoid	Length	l_3	6.67×10^{-2} m	DigiMorph Staff 2004
	Height	h_3	6.5×10^{-4} m	DigiMorph Staff 2004
	Width	w_3	6.5×10^{-4} m	DigiMorph Staff 2004
	Density[e]	ρ_3	1200 kg m^{-3}	Oda *et al* 2006
	Young's modulus[f]	E_3	1.5×10^9 Pa	Alexander *et al* 1977
	Damping coefficient[e]	ζ	0.25	Revel *et al* 2003
Skull bone with cerebrospinal fluid (CSF)	Diameter	d_4	2×10^{-2} m	DigiMorph Staff 2004
	Thickness	t_4	2.5×10^{-3} m	DigiMorph Staff 2004
	Density	ρ_4	1456 kg m^{-3}	Oda *et al* 2006
	Young's modulus	E_4	8.75×10^9 Pa	Oda *et al* 2006
	Poisson's ratio	ν	0.2	Oda *et al* 2006
	CSF viscosity[g]	μ	8.5×10^{-4} N·s m^{-1}	Oda *et al* 2006
Brain	Diameter	d_5	1.5×10^{-2} m	DigiMorph Staff 2004
	Density	ρ_5	1040 kg m^{-3}	Oda *et al* 2006

[a] Calculated from the drumming frequency.
[b] Data from woodpecker cranium.
[c] Data from toucan beak.
[d] Data from human skull bone.
[e] Data from human tendon.
[f] Data from mammal tendon.
[g] Data from human CSF.

this analysis does not consider the spongy bone, a major role of the spongy bone in drumming is expected to attenuate incident mechanical excitations with frequencies higher than a specific frequency. The sponge-like bone within the skull bone is a porous material with resilience rigidity which makes its mechanical vibration analysis too complicated. The skull bone is therefore characterized by an empirical method.

3.3. Empirical analysis of spongy bone

In a woodpecker, the mechanical excitations generated from drumming are also cushioned by the spongy bone. This sponge-like bone is known to distribute the mechanical excitations before they propagate to the brain. However, to the best of our knowledge, there has been no quantitative characterization on the shock-absorbing characteristics of the spongy bone, and a lumped parameter model for the spongy bone has been still in great uncertainty. The spongy bone is therefore characterized in an empirical way.

For this purpose, five kinds of close-packed SiO_2 microglasses whose average diameters are respectively 68, 120, 375, 500, and 875 μm were prepared, mimicking a porous structure with the resilience rigidity of the woodpecker's spongy bone. As shown in figure 7(*a*), the five kinds of microglasses closely filled an aluminum enclosure with a particle-filling ratio of 62.5% which is known to be the maximum particle-filling ratio when single-sized microglasses are packed into a container under external tapping (McGeary 1961). Figure 7(*b*) shows an experimental setup composed of close-packed microglasses, an aluminum enclosure, a vibration exciter, a power amplifier, a signal generator, reference and measurement accelerometers, and a data recorder. The aluminum enclosure containing close-packed microglasses and measurement accelerometer was vertically and randomly vibrated by the vibration exciter whose vibration condition was 10 g and up to 25 kHz. The measurement accelerometer embedded in the microglasses measured the transmitted mechanical excitations through the close-packed microglasses, whereas the reference one placed on the top surface of the aluminum enclosure measured the applied mechanical excitations.

The output signal of the measurement accelerometer was compared to that of the reference one to investigate the shock absorption by the close-packed microglasses. Figure 8(*a*) shows the measured vibration transmissibility T_v which is described as $T_v = u_{mea}/u_{ref}$, where u_{mea} and u_{ref} are the

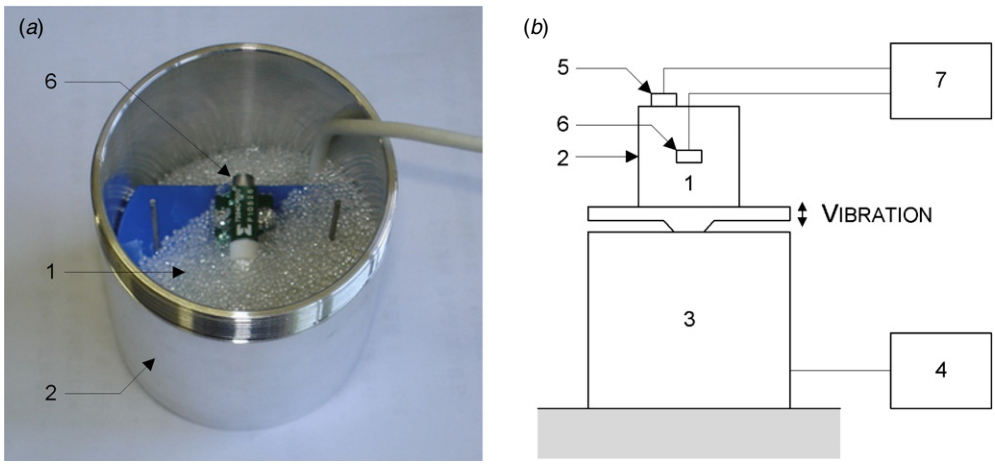

Figure 7. Experimental setup for empirical characterization of the spongy bone. (*a*) Enlarged view of the aluminum enclosure, showing microglasses and a reference accelerometer. (*b*) Experimental apparatus consisting of (1) microglasses, (2) aluminum enclosure, (3) vibration exciter, (4) power amplifier and signal generator, (5) reference accelerometer, (6) measurement accelerometer, (7) data recorder.

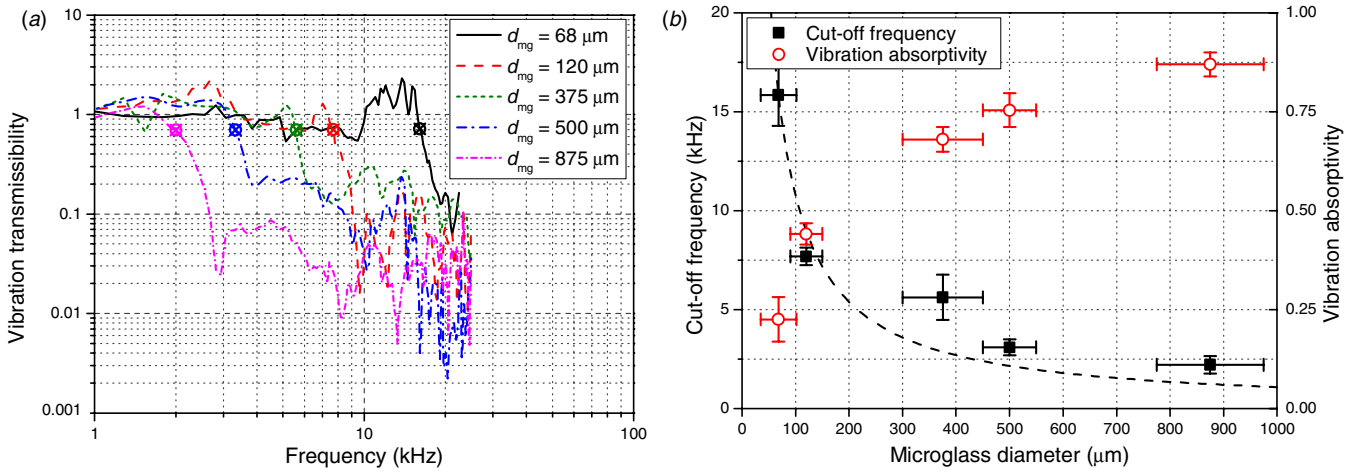

Figure 8. Empirical characterization results of the spongy bone, obtained by using close-packed microglasses, showing its shock-absorbing effect (low-pass filter effect). (*a*) Measured vibration transmissibility as a function of frequency for microglasses with average diameters of 68, 120, 375, 500, and 875 μm. (*b*) Measured cut-off frequency and vibration absorptivity as a function of microglass diameter.

output values measured from measurement and reference accelerometers at each sampling frequency, respectively. The measured vibration transmissibility shows the porous structure with resilience rigidity absorbs mechanical excitations with higher frequency than a cut-off frequency which is determined by the diameter of the microglasses. From the vibration transmissibility result, the cut-off frequency and vibration absorptivity of each kind of microglass were obtained. The cut-off frequency is a frequency at which the ratio of the output signal to the input signal is 0.707, and the vibration absorptivity is a ratio of the dissipated energy to the input energy. The dependences of the cut-off frequency and vibration absorptivity on the diameter of the microglasses are shown in figure 8(*b*). The cut-off frequency f_c is inversely proportional to the diameter of the microglasses d_{mg} which is written by $f_c = \chi \cdot d_{\mathrm{mg}}{}^{-1}$ where χ is a constant whose value is determined as 1076.9 kHz μm (Yoon and Kim 2006, Yoon *et al* 2009). Similar to the close-packed microglasses, the woodpecker's spongy bone is believed to transmit 90–99% lower frequency and to absorb 90–99% higher frequency than the spongy bone's cut-off frequency through resonant scattering and Rayleigh scattering. The spongy bone is therefore thought to perform a low-pass filtering function and also a shock-attenuating function.

4. Bio-inspired shock-absorbing system

4.1. Design and fabrication

The shock-absorbing mechanism of the woodpecker suggests that the *g*-force tolerance of micromachined devices can be improved by: (i) an external layer with high strength which protects the micromachined devices from physical damage (e.g. deformation, fracture, etc) like the woodpecker's beak; (ii) a viscoelastic layer which evenly distributes incident mechanical excitations like the hyoid; (iii) a porous structure with resilience rigidity which suppresses high-frequency mechanical excitations and prevents transmitted ones from being concentrated into the micromachined devices like the spongy bone; (iv) another high-strength layer which

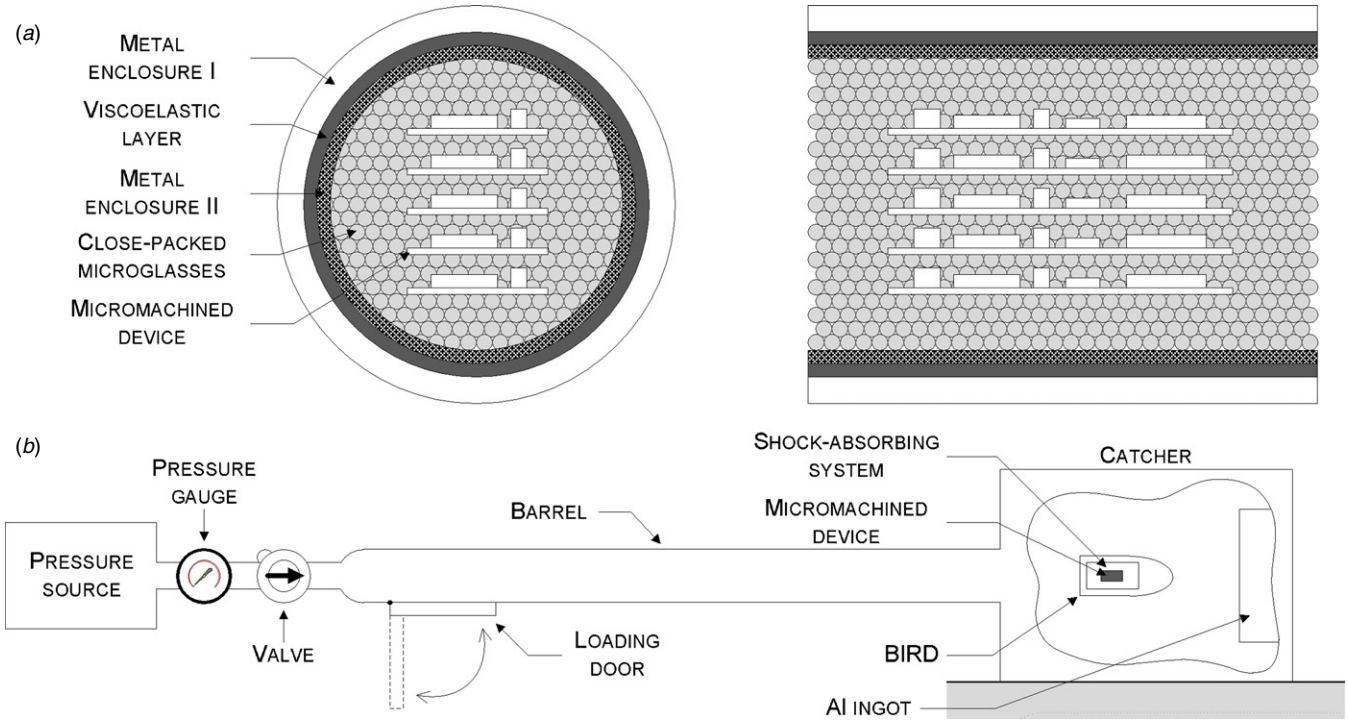

Figure 9. Bio-inspired shock-absorbing system to improve the *g*-force tolerance of micromachined devices for their high-*g* applications. (*a*) Schematic of the bio-inspired shock-absorbing system. (*b*) Experimental setup for a 60 mm air-gun experiment to characterize the bio-inspired shock-absorbing system.

contains a porous structure like the skull bone. The shock-absorbing mechanism of a woodpecker is translated into a bio-inspired shock-absorbing system to protect micromachined devices from mechanical excitations, based on the analogical conversion summarized in table 3. In this conversion, the beak, hyoid, spongy bone, and skull bone with CSF of a woodpecker correspond to a metal enclosure I, a viscoelastic material layer, close-packed microglasses, and a metal enclosure II of the bio-inspired shock-absorbing system, respectively. Figure 9(*a*) shows the bio-inspired shock-absorbing system to improve the *g*-force tolerance of micromachined devices. The metal enclosure I protects other components from external damage and applies pre-compression on the viscoelastic layer with the metal enclosure II by fastening them together. Secondly, the viscoelastic layer awards resilience to the bio-inspired shock-absorbing system and impedes the amplification of the incident mechanical excitations through pre-compression. The metal enclosure II provides a space for the close-packed microglass and prevents the internal flow of the close-packed microglass within itself. Finally, the close-packed microglass with a great number of air gaps pack micromachined devices tightly, thereby absorbing short-duration mechanical excitations in a kinetic way.

In the bio-inspired shock-absorbing system, the main design factors are the material and dimension of each component and the particle-filling ratio of the close-packed microglass. The materials and thicknesses of the metal enclosures I and II are designed to prevent their deformation under mechanical excitations. A hardened steel case with 3 mm thickness and 60 mm outer diameter is designed for the metal enclosure I and an aluminum case with 1 mm thickness and 50 mm outer diameter is used for the metal enclosure II, thereby securing at least 5 mm gap between metal enclosure II and micromachined devices. The viscoelastic layer made of rubber is designed to have 2.5 mm thickness and 50 mm inner diameter, which means that its outer diameter is changed from 55 to 54 mm through pre-compression by metal enclosures I and II. For the close-packed microglass, SiO_2 beads with a diameter of 375 ± 75 μm are filled into the metal enclosure II under mallet tapping to achieve a particle-filling ratio of about 62.5%. Micromachined devices are therefore floated in the middle of the close-packed microglass.

Table 3. Analogy between a woodpecker and a bio-inspired shock-absorbing system.

Woodpecker (*Melanerpes aurifrons*)	Bio-inspired shock-absorbing system
Beak	Metal (steel) enclosure I
Hyoid	Viscoelastic layer (rubber)
Spongy bone	Close-packed microglass
Skull bone with CSF	Metal (aluminum) enclosure II
Brain	Micromachined devices

4.2. 60 m smoothbore air-gun experiment

A 60 mm air-gun experiment was carried out to explore the *g*-force tolerance improvement of commercial micromachined devices by a bio-inspired shock-absorbing system, compared to that by hard resin (3M Scotchcast^{TM}) in high-*g* environment of up to 60 000 *g*. The 60 mm air-gun consisting of a pressure source, a pressure gauge, a valve, a barrel, and a catcher with

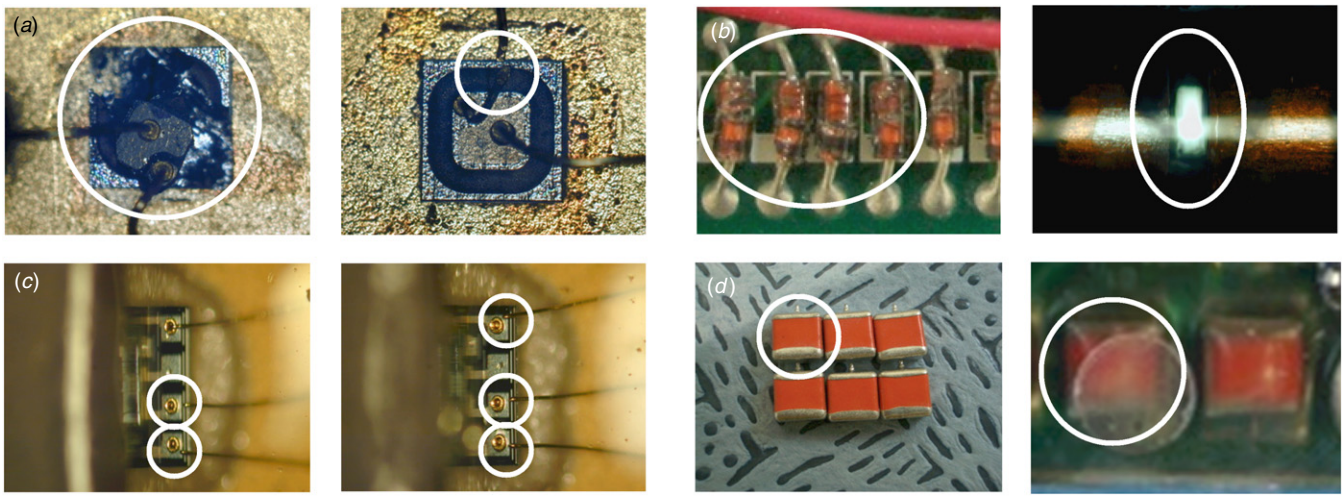

Figure 10. Failures of the micromachined devices protected by the hard resin after a 60 mm air-gun experiment. (*a*) Substrate delamination failure of SCR. (*b*) Discontinuity failure of a diode. (*c*) Bonding-wire open failure of an optocoupler. (*d*) Dielectric layer failure of a capacitor.

Table 4. 60 mm air-gun experiment results of the bio-inspired shock-absorbing system, compared to those of the hard resin shock-absorbing system.

		Failure rate (%)											
		Bio-inspired shock-absorbing system						Hard resin shock-absorbing system					
Device	Package type	20 000 *g*		40 000 *g*		60 000 *g*		20 000 *g*		40 000 *g*		60 000 *g*	
SCR	Lead	0	(0/36)	0	(0/36)	0	(0/36)	0	(0/36)	0	(0/36)	13.9	(5/36)
	SMD	0	(0/28)	0	(0/28)	0	(0/28)	0	(0/28)	0	(0/28)	0	(0/28)
Diode	Lead	0	(0/144)	0	(0/144)	0.7	(1/144)	0	(0/144)	5.6	(8/144)	26.4	(38/144)
	SMD	0	(0/104)	0	(0/104)	0	(0/104)	0	(0/104)	0	(0/104)	9.6	(10/104)
Optocoupler	DIP	0	(0/48)	0	(0/48)	0	(0/48)	0	(0/48)	6.3	(3/48)	22.9	(11/48)
Capacitor	SMD	0	(0/44)	0	(0/44)	0	(0/44)	0	(0/44)	0	(0/44)	6.8	(3/44)

an aluminum ingot was used to introduce high-*g* mechanical excitations, as shown in figure 9(*b*). The tested micromachined devices were silicon-controlled rectifiers (SCRs), diodes, optocouplers, and capacitors which are known to be sensitive to mechanical excitations. Information about the micromachined commercial devices is as follows: lead-type SCRs (PN: 2N2324), surface mount device (SMD)-type SCRs (PN: MCR703A), lead-type diodes (PN: 1N965), SMD-type SCRs (PN: MMBZ5221BLT1), dual inline package (DIP)-type optocouplers (PN: 5962-8978501ZA), and SMD-type capacitors (PN: 595D127×0020R7T).

A BIRD-I using a hard resin shock-absorbing system which contains the micromachined devices in the hard resin was tested as a control experiment. In the 60 mm air-gun experiment, the above micromachined devices embedded in the hard resin were exposed to mechanical excitations of 20 000 to 60 000 *g*. The tested micromachined devices had the physical failures of substrate delamination in the SCRs, discontinuity in the diodes, bonding-wire open in the optocouplers, and dielectric layer breakdown in the capacitors, as shown in figure 10. This hard resin shock-absorbing system successfully protected the micromachined devices up to 40 000 *g*, but made 26.4% of them physically damaged at 60 000 *g*. The measured failure rate of the hard resin shock-absorbing system, the ratio of the number of failed devices to the number of tested devices, is summarized in table 4.

A BIRD-II using a bio-inspired shock-absorbing system, which contains the micromachined devices within the close-packed microglass was also examined under the same conditions to compare the bio-inspired shock-absorbing system to the hard resin one in terms of the shock survivability of the micromachined devices. In the bio-inspired shock-absorbing system, almost all the micromachined devices survived at a high-*g* mechanical excitation of 60 000 *g*. This is because high-frequency mechanical excitations corresponding to the resonance frequencies of the micromachined devices are absorbed by the bio-inspired shock-absorbing system and even the transmitted mechanical excitations are detoured around the micromachined devices. As shown in table 4, the bio-inspired shock-absorbing system is superior to a hard resin shock-absorbing system in improving the *g*-force tolerance of commercial micromachined devices.

5. Conclusions

The advanced shock-absorbing mechanism of a woodpecker has been analyzed to develop a new class of bio-inspired

shock-absorbing system which improves the g-force tolerance of micromachined devices at high-g and high-frequency mechanical excitations. The woodpecker dissipates the mechanical excitations generated from drumming with its unique endoskeletal structures such as its beak, hyoid, spongy bone, and skull bone. To understand the woodpecker's special shock-absorbing mechanism, which cannot be explained merely by allometric scaling, those head structures have been studied in mechanical vibration and experimental methods on the basis of x-ray computed tomography images. From these analyses, the bio-inspired shock-absorbing system consisting of close-packed microglasses, viscoelastic layer, and metal enclosures with fasteners has been successfully designed, fabricated, and characterized to suppress unwanted high-g and high-frequency mechanical vibrations, thereby effectively protecting commercial micromachined devices from external mechanical excitations. In the experimental study using a 60 mm smoothbore air-gun, the bio-inspired shock-absorbing system has reduced remarkably the failure rate of micromachined devices to 0.7% at 60 000 g, whereas 26.4% of micromachined devices were physically damaged with the conventional hard-resin method.

Acknowledgments

The authors would like to thank Tomas W P Slatin (TomSlatin.com) and the DigiMorph Staff (The Digital Morphology Library) for their photo contributions. We thank Taekwon Jee for his help in preparing this paper.

References

Alexander R M and Bennet-Clark H C 1977 Storage of elastic strain energy in muscle and other tissues *Nature* **265** 114–7

Bloomfielda I G, Johnstona I H and Bilstonb L E 1998 Effects of proteins, blood cells and glucose on the viscosity of cerebrospinal fluid *Pediatr. Neurosurg.* **28** 246–51

Britan A, Ben-Dor G, Igra O and Shapiro H 2001 Shock wave attenuation by granular filters *Int. J. Multiphase Flow* **27** 617–34

Burton R R 1988 G-induced loss of consciousness: definition, history, current status *Aviat. Space Environ. Med.* **59** 2–5

Chu A S 1988 Built-in mechanical filter in a shock accelerometer *Proc. 59th Shock and Vibration Symp.* pp 251–67

Dareing D W and Johnson K L 1975 Fluid film damping of rolling contact vibrations *J. Mech. Eng. Sci.* **17** 214–8

DigiMorph Staff 2004 *Melanerpes aurifrons* (online Digital Morphology) http://digimorph.org/specimens/Melanerpes_aurifrons/

Fortis A P, Kostopoulos V, Panagiotopoulos E, Tsantzalis S and Kokkinos A 2004 Viscoelastic properties of cartilage-subchondral bone complex in osteoarthritis *J. Med. Eng. Technol.* **28** 223–6

Friend R D and Kinra V K 2000 Particle impact damping *J. Sound Vib.* **233** 93–118

Gibson L J 2006 Woodpecker pecking: how woodpeckers avoid brain injury *J. Zool.* **270** 462–5

Grover A S and Kapur A D 1982 Shock response of viscoelastically damped sandwich plates *J. Sound Vib.* **85** 355–64

Koiter W T 1963 *Progress in Applied Mechanics* (New York: MacMillan)

May P R A, Fuster J M, Newman P and Hirschman A 1976a Woodpeckers and head injury *Lancet* **307** 454–5

May P R A, Fuster J M, Newman P and Hirschman A 1976b Woodpeckers and head injury *Lancet* **307** 1347–8

McGeary R K 1961 Mechanical packing of spherical particles *J. Am. Ceramic Soc.* **44** 513–22

Moore J R and Maguire D A 2004 Natural sway frequencies and damping ratios of trees: concepts, review and synthesis of previous studies *Trees—Structure and Function* **18** 195–203

Moore K L and Dalley A F 2005 *Clinically Oriented Anatomy* (New York: Williams & Wilkins)

Nakra B C 1976 Vibration control with viscoelastic materials *Shock Vib. Dig.* **8** 3–12

Nakra B C 1981 Vibration control with viscoelastic materials: II *Shock Vib. Dig.* **13** 17–20

Nakra B C 1984 Vibration control with viscoelastic material: III *Shock Vib. Dig.* **16** 17–22

Nashif A D, Jones D I G and Henderson J P 1985 *Vibration Damping* (New York: Wiley)

Oda J, Sakamoto J and Sakamoto K 2006 Mechanical evaluation of the skeletal structure and tissue of the woodpecker and its shock absorbing system *JSME Int. J.* A **49** 390–6

Panossian H V 1991 An overview of NOPD: a passive damping technique *Shock Vib. Tech. Rev.* **1** 4–10

Panossian H V 1992 Structural damping enhancement via non-obstructive particle damping technique *J. Vib. Acoust.* **114** 101–5

Parent A 1996 *Carpenter's Human Neuroanatomy* (New York: Williams & Wilkins)

Ping Y 2007 Design and dynamic practice of a novel fluid vibration isolator for packaging protection of electronic equipment *J. ASTM Int.* **4** JAI101088

Reissner E 1946 Stresses and small displacements of shallow spherical shells-I *J. Math. Phys.* **25** 80–5

Revel G M, Scalise A and Scalise L 2003 Measurement of stress-strain and vibrational properties of tendons *Meas. Sci. Technol.* **14** 1427–36

Schwab I R 2002 Cure for a headache *Br. J. Ophthalmol.* **86** 843–6

Seki Y, Schneider M S and Meyers M A 2005 Structure and mechanical behavior of a toucan beak *Acta Mater.* **53** 5281–96

Stark R D, Dodenhoff D J and Johnson E V 1998 A quantitative analysis of woodpecker drumming *Condor* **100** 350–6

Veprik A M and Babitsky V I 2000 Vibration protection of sensitive electronic equipment from harsh harmonic vibration *J. Sound Vib.* **238** 19–30

Vincent J F D, Sahinkaya M N and O'Shea W 2007 A woodpecker hammer *Proc. Inst. Mech. Eng.* C **221** 1141–7

Vogl S 1998 *Cats' Paws and Catapults* (New York: Norton)

Whinnery J E and Whinnery A M 1990 Acceleration-induced loss of consciousness: a review of 500 episodes *Arch. Neurol.* **47** 764–76

Yazdi N, Ayazi F and Najafi K 1998 Micromachined inertial sensors *Proc. IEEE* **86** 1640–59

Yoon S-H and Kim K L 2006 Passive low pass filtering effect of mechanical vibrations by a granular bed composed of microglass beads *Appl. Phys. Lett.* **89** 021906

Yoon S-H, Roh J-E and Kim K L 2009 Woodpecker-inspired shock isolation by microgranular bed *J. Phys. D: Appl. Phys.* **42** 035501